Mechanics of Cutaneous Wound Rupture

Digendranath Swain[a], Anurag Gupta[a,*]

[a] *Department of Mechanical Engineering,*
Indian Institute of Technology,
Kanpur, India, 208016

Abstract

A cutaneous wound may rupture during healing as a result of stretching in the skin and incompatibility at the wound-skin interface, among other factors. By treating both wound and skin as hyperelastic membranes, and using a biomechanical framework of interfacial growth, we study rupturing as a problem of cavitation in nonlinear elastic materials. We obtain analytical solutions for deformation and residual stress field in the skin-wound configuration while emphasizing the coupling between wound rupture and wrinkling in the skin. The solutions are analyzed in detail for variations in stretching environment, healing condition, and membrane stiffness.

Keywords: Cutaneous wound healing, Wound rupture, Residual stress, Interfacial growth, Wrinkling, Cavitation

1. Introduction

The physiological, cytological, and dehiscence characteristics of cutaneous wound healing are all well researched in the biology literature (Singer and Clark, 1999; Broughton and Rohrich, 2005; Gurtner et al., 2008; Grinnell, 1994; Hahler, 2006; Harhap, 1993). On the other hand, mathematical modelling of wound healing has been conventionally restricted to mostly the biochemical aspects of the problem invoking reaction-diffusion equations for various cellular processes and growth factors (Murray, 2003). Subsequently, however, the importance of mechanical forces and elasticity in restoring the integrity of damaged skin tissues was established (Murray, 2003; Agha et al., 2011; Gurtner et al., 2008; Evans et al., 2013) leading to several proposals of mechanistic models of wound healing (Hall, 2008; Murphy et al., 2011; Tranquillo and Murray, 1992). It has been only recently that cutaneous wound healing is being explored as a problem of biomechanical growth with both skin and the wound modelled as nonlinear elastic materials (Swain and Gupta, 2015; Wu and Amar, 2015; Bowden et al., 2016). The nonlinearity in the elastic response leads to mechanical instabilities in the form of irregular wound geometries (Wu and Amar, 2015), wrinkling in the skin surrounding the wound (Swain and Gupta, 2015) (see also Cerda (2005); Flynn and McCormack (2008); Li and Wang (2011)), and, as shown in the present paper, cavitation in the wound. An understanding of the biomechanics behind such instabilities can provide valuable insights into scar formation and wound management. To the best

*Corresponding author
Email address: `ag@iitk.ac.in` (Anurag Gupta)

of our knowledge, wound cavitation has not been incorporated in any of the previous mathematical models of cutaneous wound closure.

The objective of our work is to study the mechanics of wound rupturing within the context of interfacial biological growth and cavitation in hyperelastic membranes. In particular, we are interested to explore the coupling between wound rupture, wrinkling in the unwounded skin, and the residual stress distribution in the skin-wound configuration. Studies in mammalian skin wounds show that the rupture strength of the wounded tissue is less than 10% of the unwounded skin within a week of wounding (Gál et al., 2006; Ramsastry, 2005). This leaves an open skin wound susceptible to rupture under sudden local stretching (Broughton and Rohrich, 2005; Gál et al., 2006). Most importantly, the rupture impairs the healing process and increases the trauma faced by the patient in addition to other health complications (Harhap, 1993). Figure 1(a) shows a ruptured wound surrounded by wrinkled unwounded skin. In our idealized mechanistic model we assume the wound geometry to be circular and consider initiation of rupture to be synonymous with void formation (cavitation) at the center of the wound, see Fig. 1(b). The void appears in the wound at some critical stretching of the skin; it is assumed to be unrelated to other forms of skin cracking such as due to dry weather and old age.

In a recent paper, we investigated the emergence of wrinkles and residual stress during wound healing using an interfacial growth model and hyperelastic Varga energies for both wound and skin (Swain and Gupta, 2015). The present work advances on to include the possibility of cavitation, which is tantamount to rupturing, in the wound. In order to do so, we propose a novel two-dimensional (2D) hyperelastic constitutive model for the wound based on a recently developed three-dimensional (3D) hyperelastic strain energy (Xin-Chung and Chang-Jun, 2001). The Varga strain energy density, used previously for the wound, prohibits cavitation and hence cannot be taken suitable for predicting rupture. In fact, cavitation in 2D elastic membranes is restricted by special constitutive requirements (Steigmann, 1992; McMahon et al., 2010; Haughton, 1986). Our model for cavitation in membranes, as a problem of existence and uniqueness of stable bifurcated solutions, follows earlier work in 3D elastic solids (Ball, 1982; Horgan and Polignon, 1995) and 2D hyperelastic membranes (Steigmann, 1992; Haughton, 2001, 1990; Haughton and McKay, 1995). The proposed framework can be used to understand the quality of scar formation, post healing, as a consequence of mechanical instabilities emerging from the nonlinear elastic nature of wound and skin. In doing so, it can form a basis for experimentally investigating the precise constitutive nature of the wound, hitherto unestablished in the literature. Our analytical solutions can also provide benchmark results for more sophisticated numerical simulations of elastic instabilities in thin films (Taylor et al., 2014, 2015; Lejeune et al., 2016b,a).

In Section 2 we formulate the kinematical structure and the governing equations for the problem at hand. Additionally, we introduce a new 2D hyperelastic strain energy density for the wound and discuss its properties and physical relevance. The boundary value problems for the unwounded skin and the wound are solved in Section 3 to obtain analytical solutions for deformations during wound closure and residual stress distributions. We also discuss criteria for initiation of mechanical instabilities in the form of wrinkling and cavitation. The obtained solutions are discussed in detail in Section 4, with an emphasis on understanding the effect of wrinkling and stretching of the unwounded skin on wound rupture and residual stress generation. We briefly discuss the possibility of cavitation at the intersecting boundary of wound and skin, before concluding our study in Section 5.

2. Problem formulation and constitutive assumptions

The purpose of this section is to develop a framework which can be used to pursue an analytical study of biomechanics of rupturing in a wound surrounded by wrinkled skin. We will formulate boundary value problems, to be solved in the next section, which yield residual stress distribution in wound-skin configuration and help us analyze the appearance as well as the effects of wrinkling and cavitation. Towards this end, we consider an instantaneous wound-skin configuration shown as $\mathcal{B}_t$ in Fig. 2, where a denotes the wound radius and b the outer radius of the skin. We model both wound and skin as 2D membranes, neglecting their thickness altogether. The deformation is assumed to be axisymmetric so that the wound-skin arrangement remains circular as wound diameter decreases during healing.

2.1. Kinematics and governing equations

We provide a quick review of kinematical relations and balance laws required for our further analysis; details can be seen in our recent work (Swain and Gupta, 2015). The deformations are measured with respect to a fixed reference configuration $\mathcal{B}_0$, see Fig. 2, where the wound and the skin regions are of radius A and B, respectively, such that $a < A$ to ensure healing. The nature of residual stresses developed during healing is determined by unloading the wound-skin configuration in $\mathcal{B}_t$ to a zero stress state. This is achieved, in the present model, by cutting and separating the configuration $\mathcal{B}_t$ along the wound edge to obtain an intermediate relaxed configuration denoted as $\mathcal{B}_i$, see Fig. 2. More quantitative details of this operation are provided later in the section. The assumed axisymmetry of interfacial growth is manifested in the axisymmetric gap between wound edge and the internal edge of the skin in $\mathcal{B}_i$.

The position vector in the reference configuration, $\mathbf{X} = R\mathbf{e}_r(\Theta) \in \mathcal{B}_0$ (with polar coordinates $0 \leq R \leq B$, and $0 \leq \Theta \leq 2\pi$), is related by a continuous bijective map to the position vector in the current configuration, $\mathbf{x} = r\mathbf{e}_r(\theta) \in \mathcal{B}_t$ (with $0 \leq r \leq b$, and $0 \leq \theta \leq 2\pi$), such that $r = r(R)$ and $\theta = \Theta$. Here, $\mathbf{e}_r$ and $\mathbf{e}_\theta$ are unit basis vectors along radial and circumferential directions of the polar coordinate system. The corresponding deformation gradient is given by

$$\mathbf{F} = r'(R)\mathbf{e}_r \otimes \mathbf{e}_r + \frac{r}{R}\mathbf{e}_\theta \otimes \mathbf{e}_\theta, \tag{1}$$

where the superscript prime is used to denote the derivative with respect to R and $\otimes$ stands for the tensor dyadic product. The nature of healing kinematics is fixed by hypothesising a piecewise continuous linear map between $\mathbf{X} \in \mathcal{B}_0$ and $\mathbb{X} \in \mathcal{B}_i$ such that $\mathbb{X} = \mathbb{R}(R)\mathbf{e}_r(\Theta)$, where $\mathbb{R}$ is given by $k_w R$ if $0 \leq R \leq A$ and $k_s R$ if $A \leq R \leq B$. The parameters k_s and k_w are morphoelastic constants for growth of the skin and annihilation of wound, respectively; they are related to mass addition at the wound-skin interface necessary for wound healing process (Swain and Gupta, 2015). The resulting growth distortion tensor is clearly isotropic, see Fig. 2, with a form

$$\mathbf{F}_g = k_i(\mathbf{e}_r \otimes \mathbf{e}_r + \mathbf{e}_\theta \otimes \mathbf{e}_\theta), \tag{2}$$

where k_i should be replaced by k_w and k_s for $0 \le R \le A$ and $A \le R \le B$, respectively. The elastic distortion tensor $\mathbf{F}_e$, satisfying the multiplicative decomposition $\mathbf{F} = \mathbf{F}_e\mathbf{F}_g$ (Rodriguez et al., 1994), can then be obtained as

$$\mathbf{F}_e = \frac{r'(R)}{k_i}\mathbf{e}_r \otimes \mathbf{e}_r + \frac{r}{k_i R}\mathbf{e}_\theta \otimes \mathbf{e}_\theta. \tag{3}$$

It is imminent from the above relation that elastic distortion $\mathbf{F}_e$ is incompatible at the wound edge unless $k_w = k_s$ (Swain and Gupta, 2015). It is this incompatibility that is manifested in the axisymmetric annular gap between wound and skin regions in $\mathcal{B}_i$. The incompatibility therefore represents the differential growth in the two domains. We require $k_s > k_w$ to ensure that the two domains do not penetrate into each other. Most importantly, the incompatibility is a source for residual stress distribution in the skin and also has a bearing on the wrinkle formation in the unwounded skin adjacent to the wound edge (Swain and Gupta, 2015).

The stress field in the wound-skin configuration satisfies equation of linear momentum balance which, for quasi-static deformations, zero body force, and axisymmetry of the problem, yields only one non-trivial equilibrium condition for stress (Haughton, 2001)

$$\frac{\mathrm{d}T_{rr}}{\mathrm{d}r} + \frac{(T_{rr} - T_{\theta\theta})}{r} = 0 \text{ for } 0 \le R < A,\ A < R \le B \tag{4}$$

such that T_{rr} is continuous at $R = A$, where $T_{rr}(R)$, etc. are components of the Cauchy stress with respect to the polar coordinate system.

2.2. Constitutive response of skin

The unwounded skin is assumed to behave like a Varga hyperelastic membrane exhibiting non-linear stress-strain response (Flynn et al., 2011). The anisotropic nature of skin is ignored for analytical simplicity whereas its viscoelasticity is neglected recognising the slow time scales involved in wound healing (Hall, 2008). It is justified to model skin as a membrane since the dermis is much softer than the epidermis allowing for skin to easily slide over the substrate (Cerda, 2005). The strain energy density (SED) of skin, as considered in the present work, is given by

$$W_s(\lambda_1, \lambda_2) = 2\mu_s\left(\lambda_1 + \lambda_2 + (\lambda_1\lambda_2)^{-1} - 3\right), \tag{5}$$

where $\mu_s > 0$ can be identified as the shear modulus of the membrane (with dimensions of force/unit length); λ_1 and λ_2 are principle stretches associated with elastic distortion. The SED in (5), for a Varga hyperelastic membrane, supports wrinkling but prohibits cavitation (Steigmann, 1992; Haughton, 2001, 1990; Haughton and McKay, 1995). It is therefore appropriate for the skin but not for the wound.

2.3. *Constitutive response of wound*

The wound is considered as a solid domain due to its granulating surface acting as a single contractile body (Broughton and Rohrich, 2005). We ignore the viscoelastic nature of the wound while modelling it as a hyperelastic membrane whose stress-strain response is less stiffer than skin due to its inferior properties. The SED function for wound is proposed as

$$W_w(\lambda_1, \lambda_2) = C_{01}(\lambda_1 + \lambda_2 - 2) + C_{02}(\lambda_1^{-1} + \lambda_2^{-1} - 2) + C_{03}(\lambda_1\lambda_2 - 1), \tag{6}$$

where C_{01}, C_{02}, and C_{03} are material constants whose physical nature will be discussed below. The 2D SED in (6) is inspired from a SED used to model cavitation in 3D compressible materials (Xin-Chung and Chang-Jun, 2001). The proposed energy density allows for cavitation in membranes, as shown in the following section. In rest of this section we analyze it further ensuring that it indeed represents a physically meaningful energy for hyperelastic membranes.

The non-trivial components of the Cauchy stress tensor for an hyperelastic response are given by (Steigmann, 1992)

$$T_{rr} = \frac{1}{\lambda_2}\frac{\partial W_w}{\partial \lambda_1} \quad \text{and} \quad T_{\theta\theta} = \frac{1}{\lambda_1}\frac{\partial W_w}{\partial \lambda_2}. \tag{7}$$

Similar expressions can be written for stresses in the skin region. The SED W_w and the derived components of Cauchy stress must vanish in the stress free configuration, i.e. when $\lambda_1 = \lambda_2 = 1$. The former of this requirement can be checked by direct substitution in (6). Regarding the latter, we first obtain the stress components using (7) as

$$T_{rr} = \frac{1}{\lambda_2}\left(C_{01} - \frac{C_{02}}{\lambda_1^2} + C_{03}\lambda_2\right) \quad \text{and} \quad T_{\theta\theta} = \frac{1}{\lambda_1}\left(C_{01} - \frac{C_{02}}{\lambda_2^2} + C_{03}\lambda_1\right). \tag{8}$$

Clearly, the requirement of stress free configuration is satisfied as long as $C_{01} - C_{02} + C_{03} = 0$. More insight on the nature of the material parameters is obtained by expanding the energy density W_w as a Taylor series in terms of the Green's strain tensor $\mathbf{E}$. The leading order terms can then be compared to the well known linear elastic constants. After retaining only linear and second order coefficients, the SED can be rewritten as

$$W_w = (C_{03}/2)(\operatorname{tr}\mathbf{E})^2 - (1/2)(C_{03} - 2C_{02})\operatorname{tr}\mathbf{E}^2 + O(\mathbf{E}^3). \tag{9}$$

Comparing this with the strain energy density for a plane stress linear elastic problem furnishes $C_{01} = \mu_w(1-2\nu)/(1-\nu)$, $C_{02} = \mu_w/(1-\nu)$, and $C_{03} = 2\mu_w\nu/(1-\nu)$, where μ_w is the shear modulus of the wound material with dimensions of force/unit length and ν is the Poisson's ratio of the material.

The principal stretches λ_1 and λ_2 are necessarily positive to prevent disappearance of material. We require energy W_w to be non-negative for any positive stretch. This is ensured by taking constants C_{01} and C_{03} to be strictly positive. These restrictions yield $\mu_w > 0$ and and $0 < \nu < 1/2$. The energy density in (6) then has a unique minima at $\lambda_1 = \lambda_2 = 1$. Moreover, the tension-extension inequalities, $\partial T_{rr}/\partial\lambda_1 > 0$ and $\partial T_{\theta\theta}/\partial\lambda_2 > 0$, are satisfied as long as $C_{02} > 0$. The energy density also satisfies the Baker-Ericksen Inequality, $(T_{rr} - T_{\theta\theta})(\lambda_1 - \lambda_2) > 0$, for positive C_{01}. The Baker-Ericksen inequality is a well established constitutive restriction for nonlinear elastic materials with important consequences for the stability and existence of solutions (Truesdell and Noll, 2004). We also note that $W_w \to \infty$ whenever principal stretches approach ∞ or $0+$. The stresses remain finite in the former limit, but tend to be unbounded for the latter. Hence, an infinite amount of stress is required to diminish material to zero volume.

We illustrate the behavior of the SED function graphically in Figs. 3(a,b) as a 2D contour map and a 3D surface plot for a fixed Poisson's ratio ($\nu = 0.3$). The uniaxial and equi-biaxial stress-stretch responses are shown in Figs. 3(c,d), respectively, for various Poisson's ratios. It can be noted that the SED has a single minima at ($\lambda_1 = 1, \lambda_2 = 1$) and the material shows some softening behavior at lower Poisson's ratios under equi-biaxial stretching.

3. Solutions for skin wrinkling and wound cavitation

In this section, we construct analytical solutions for deformation and residual stress in skin-wound configuration. We will first consider the case of unwrinkled skin and then use tension field theory to derive solutions in the wrinkled region of the skin. Following these we will obtain the solution in the wound region allowing for the possibility of cavitation at the center of the wound. We will also show that, beyond a critical bifurcation point, the cavitation solution is always stable and would be preferred over the homogeneous solution without any cavitation.

3.1. Solution for unwrinkled skin

The stress fields in the skin can be computed using relations (7), but with SED given by (5), as

$$T^s_{rr} = 2\frac{\mu_s}{\lambda_2}\left(1 - \frac{1}{\lambda_1^2\lambda_2}\right) \quad \text{and} \quad T^s_{\theta\theta} = 2\frac{\mu_s}{\lambda_1}\left(1 - \frac{1}{\lambda_1\lambda_2^2}\right), \tag{10}$$

where the superscript 's' is used to indicate their connection with skin. Substituting these in (4), with $\lambda_1 = r'/k_s$ and $\lambda_2 = r/(k_s R)$ from (3), we obtain a second order ordinary differential equation (ODE) $r''rR + (r')^2R - r'r = 0$, which has a straightforward solution $r(R) = \sqrt{C_1R^2 + C_2}$, with constants C_1 and C_2 to be determined from two boundary conditions. First, we consider $r(B) = b$ to be known, which is equivalent to prescribing the circumferential stretch at the outer boundary. Second, we also assume $r(A) = a = \zeta A$ to be given from the healing conditions of the wound, where ζ is the healing constant (Swain and Gupta, 2015). For a healing wound $\zeta < 1$ and for an atrophic wound $\zeta > 1$. The unknown constants can then be calculated as $C_1 = (b^2 - a^2)/(B^2 - A^2)$ and $C_2 = (a^2B^2 - b^2A^2)/(B^2 - A^2)$. They can be rewritten in terms of the circumferential stretch at the outer boundary, denoted by λ_{2B}, and a dimensionless parameter $\alpha = B/A$ as $C_1 = \left((\lambda_{2B}k_s\alpha)^2 - \zeta^2\right)/(\alpha^2 - 1)$ and $C_2 = \left(\zeta^2 - (\lambda_{2B}k_s)^2\right)\alpha^2A^2/(\alpha^2 - 1)$. The constants are expressed in terms of four physical parameters, ζ, k_s, λ_{2B}, and α, whose prescription is necessary for the complete solution. The above solution is physically meaningful as long as the associated stress fields remain non-negative. Indeed, ideal membranes cannot support compressive stresses and instead wrinkle to accommodate the compression causing slackness. The solution which allows for partially wrinkled skin is discussed next.

3.2. Wrinkled skin and tension field theory

We now look for a solution where the skin region, $A \le R \le B$, has been partially wrinkled in a domain, $A \le R \le R_c$, adjacent to the wound (see also Swain and Gupta (2015)). The radius R_c denotes the boundary between wrinkled and unwrinkled skin. The wrinkling will be circumferential in nature, as shown in Fig. 1(b), if the radial stress remains positive throughout and only the hoop stress, when calculated in Section 3.1, becomes compressive for $A \le R \le R_c$. Our simplistic model cannot reveal the wavelength of the wrinkling pattern due to vanishing bending rigidity of the membrane. The solution obtained in the previous section remains valid in the unwrinkled part of the skin, although with different expressions of C_1 and C_2. For circumferential wrinkling to appear, the hoop stress $T^s_{\theta\theta}$ must monotonically increase from the inner edge of the skin, where they take a compressive value, to the outer edge while changing its sign at $R = R_c$. The monotonicity of the hoop stress can be checked by calculating the gradient, using results in Section 3.1, $(T^s_{\theta\theta})' = -2\mu_s C_2 k_s/(C_1 R^2 r)$. Note that, since $\lambda_1 = C_1 R/r k_s$ and $\lambda_1 > 0$, we require $C_1 > 0$. As a result, for circumferential wrinkling to exist, we should have $C_2 < 0$. Additionally, these constants should be such that T_{rr} remains positive throughout. The radius R_c can be obtained by solving for R in $T_{\theta\theta} = 0$, which yields a nonlinear algebraic equation $\mathrm{C}_1\sqrt{\mathrm{C}_1 R_c^2 + \mathrm{C}_2} = k_s^3 R_c$. Wrinkling can be avoided as long as $R_c \le A$ or equivalently when $k_s^3 \ge (b^2 - a^2)\zeta/(B^2 - A^2)$.

In order to find the solution in the wrinkled region, $A \le R \le R_c$, we use tension field theory as proposed by Pipkin and Steigmann (Pipkin, 1986; Steigmann, 1990). The essential idea is to regularise the original energy to obtain a relaxed energy which is compatible with the wrinkled solution. The 'natural width' $n(\lambda_1)$ of the membrane is given by λ_2 which can be solved in terms of λ_1 using $T^s_{\theta\theta} = 0$ to obtain $\lambda_2 = 1/\sqrt{\lambda_1}$ (Pipkin, 1986; Haughton and McKay, 1995). The relaxed SED function, denoted by W_s^*, is defined as

$$W_s^*(\lambda_1) = W_s(\lambda_1, n(\lambda_1)) = 2\mu_s \left(\lambda_1 + 2/\sqrt{\lambda_1} - 3\right), \tag{11}$$

where we have used superscript $*$ to indicate the tension field variables. The governing equation (4) simplifies to $\mathrm{d}T^*_{rr}/\mathrm{d}r + T^*_{rr}/r = 0$ yielding $rT^*_{rr} = \text{const.}$, which in conjunction with $(10)_1$ gives $R(1 - \lambda_1^{-1.5}) = \text{const}$. This can be integrated to calculate the deformation in the wrinkled region as (Haughton and McKay, 1995; Swain and Gupta, 2015)

$$r^*(R) = \int \left(\frac{R}{R - \delta_1}\right)^{2/3} k_s \mathrm{d}R + \delta_2, \tag{12}$$

where δ_1 and δ_2 are constants. The four unknown constants, δ_1, δ_2 in the wrinkled solution and C_1, C_2 in the unwrinkled solution, can be determined from two boundary conditions given by the continuity of deformation and radial stress at wrinkle boundary $R = R_c$ apart from two other boundary conditions prescribing displacements at the inner and the outer edge of the skin domain, as in Section 3.1.

3.3. Solution allowing for cavitation in the wound

The governing equation for deformation in the wound region can be obtained by substituting stresses from (8) into (4), and using $\lambda_1 = r'/k_w$ and $\lambda_2 = r/(k_w R)$, as

$$2r^2 R r'' - r^2 r' + R^2 (r')^3 = 0. \tag{13}$$

To solve the preceding second order ODE, we need two boundary conditions. Towards this end, we prescribe displacement at the wound edge $r(A) = k_w \lambda A$, where λ is the applied stretch transmitted through the skin (or equivalently through the wound edge stresses). The second boundary condition is given by $r(0) = 0$ when no cavity appears at the center of the wound domain, or $r(0^+) = \gamma > 0$ when a cavity (or void) appears at the center. In the latter scenario, the surface of the cavity must be traction free, i.e. $T_{rr}(0^+) = 0$ (Steigmann, 1992). A solution with homogeneous deformation of the kind $r = k_w \lambda R$ satisfies (13) and the boundary conditions without cavity. We are however interested in finding a solution which allows for cavity. To do so, we introduce $\beta(R) = \lambda_1/\lambda_2 = Rr'/r$ and rewrite (13) as $2R\beta' + \beta(\beta - 1)(\beta + 3) = 0$. The first order ODE can be integrated to obtain $R(\beta) = D\beta^{2/3}(\beta + 3)^{-1/6}/\sqrt{\beta - 1}$ and $r(\beta) = C\sqrt{\beta + 3}/\sqrt{\beta - 1}$, where D and C are constants of integration, to be determined using $R(\beta_A) = A$ and $r(\beta_A) = k_w \lambda A$, where $\beta_A = \beta(A)$. After solving for these constants we obtain

$$R(\beta) = A\left(\frac{\beta}{\beta_A}\right)^{2/3}\left(\frac{\beta_A + 3}{\beta + 3}\right)^{1/6}\left(\frac{\beta_A - 1}{\beta - 1}\right)^{1/2} \quad \text{and} \tag{14}$$

$$r(\beta) = k_w \lambda A\left(\frac{\beta + 3}{\beta_A + 3}\right)^{1/2}\left(\frac{\beta_A - 1}{\beta - 1}\right)^{1/2}. \tag{15}$$

The parameter β can be eliminated between these two expression to find the deformation $r(R)$ in the wound. The constant β_A will be determined below. Due to the positivity of the principal stretches, $\beta > 0$. Also, for finite $r(R = 0^+)$, $\beta(0^+) = 0$. Hence, for the cavitation solution, $0 < \beta < 1$, since otherwise $\beta' < 0$ which leads to a contradictory result. This also necessitates $0 < \beta_A < 1$. At the center of the wound (15) yields

$$\gamma = k_w \lambda A\sqrt{3(1 - \beta_A)}/\sqrt{\beta_A + 3}. \tag{16}$$

We can study the cavitation phenomenon as a bifurcation problem. Indeed, there is a critical value of the stretch λ, controlled at the wound edge, at which the cavitation solution exists; the critical value, denoted as λ_c, will be calculated below. For $\lambda < \lambda_c$, only the homogeneous solution (without cavity) is possible and there is no solution which allows for a cavity at the center of the wound. On the other hand, for $\lambda > \lambda_c$ it is possible to obtain another solution which allows for cavitation. We will identify $\lambda = \lambda_c$ as the critical point for bifurcation. As we shall see later in the section, the cavitation solution is energetically stable and will therefore be preferred over the homogeneous solution beyond the critical point. In order to find λ_c, we begin by noting that $\gamma = 0$ at the critical point of bifurcation, which can be used to calculate the critical value of β_A as $\beta_{Ac} = 1$. The critical stretch λ_c will be obtained using the stress free boundary condition at $R = 0$ (i.e. on the edge of cavity). First, using (14) and

(15), we write principle stretches as $\lambda_2 = \lambda(\beta_A/\beta)^{2/3}(\beta+3)^{2/3}(\beta_A+3)^{-2/3}$ and $\lambda_1 = \beta\lambda_2$, which are then substituted into the expression for radial stress in $(8)_1$. The traction free boundary condition $T_{rr}(0) = 0$, on using $\beta = 0$ at R=0, immediately yields $-C_{02}(3+\beta_A)^2 + 9\lambda^3\beta_A^2 C_{03} = 0$. Recalling that $C_{03} = 2\nu C_{02}$, we can solve this equation to obtain a formula for β_A as $\beta_A = 3/\left(3\sqrt{2\nu\lambda^3} - 1\right)$. Furthermore, using $\beta_{Ac} = 1$ gives the critical value of stretch, $\lambda_c = 2(9\nu)^{-1/3}$. Interestingly, the critical stretch depends only on the Poisson's ratio. The derived relation for β_A can be used in (16) to get an expression for the size of the cavity,

$$\gamma = k_w \lambda A \sqrt{1 - 4/(3\sqrt{2\nu\lambda^3})}. \tag{17}$$

The variation in β_A with respect to applied stretch for various Poisson's ratios is shown in Fig. 4(a). The intersection of $\beta_A = 1$ line with the plotted curves provide the critical stretch for the respective Poisson's ratio. For any stretch applied beyond these points, β_A diminishes non-linearly. In Fig. 4(b) we illustrate void growth with respect to the applied stretch. Clearly, the growth, as well as the critical stretch at which growth initiates, varies with Poisson's ratio of the wound material.

Finally, we verify whether cavitation is energetically stable for edge stretch magnitudes beyond the critical value. The total stored energy of the axisymmetrically deforming circular wound is given by $E = \int_0^A 2\pi W_w R \mathrm{d}R$. Its evaluation is greatly simplified by noting an identity, $2RW_w = \left(R^2(W_w - (\lambda_1 - \lambda_2)\partial W_w/\partial\lambda_1)\right)'$, which can be verified using (3), (4), and (7). As a result, the total energy reduces to $E = \pi A^2(W_w - (\lambda_1 - \lambda_2)\partial W_w/\partial\lambda_1)$, where all the fields are evaluated at $R = A$. Using the energy density W_w as postulated in (6), we first calculate the total energy for the homogeneous solution, i.e. when $\lambda_1 = \lambda_2 = \lambda$, as $E_{hom} = \pi A^2(\lambda - 1)^2(2C_{02}/\lambda + C_{03})$. Analogously, we can obtain the total energy for the non-homogenous cavitation solution, where at the wound edge $\lambda_1 = \beta_A\lambda$ and $\lambda_2 = \lambda$, as

$$E_{nonhom} = \pi A^2\left((\lambda-1)^2 C_{03} + C_{02}\left(2(\lambda-2) + \frac{2\beta_A + \beta_A^2 - 1}{\lambda\beta_A^2}\right)\right). \tag{18}$$

The difference $E_{hom} - E_{nonhom} = \pi A^2 C_{02}(\beta_A - 1)^2/\lambda\beta_A^2$ is always positive since $\lambda > 0$ and $C_{02} > 0$. Therefore the cavitation solution is energetically favourable over the homogeneous solution.

4. Discussion

We are broadly interested in three phenomena during rupture of a cutaneous wound: wrinkle formation in the skin adjacent to the wound, emergence of residual stresses in the skin due to wound healing and wound edge incompatibility, and void formation in the wound as a result of cavitation in the wound membrane. The hyperelastic membrane models for skin and wound, as proposed in the previous section, allow for these occurrences. We will now discuss in detail the physical nature of our model as well as the solutions, and study their dependence on various parameters. To begin with, we plot (in Fig. 5) radial and hoop stresses derived from the Varga model of skin given in (5). We fix $\alpha = B/A = 3$ and obtain stress distributions for varying incompatibility parameter k_s, healing constant ζ, and applied stretch λ_{2B}. The skin domain is stress free when all the parameters are unity. For all other considered values, the circumferential stress takes negative values in a finite region, indicating the emergence of wrinkling. The stress fields in the wrinkled region need to be modified using tension field theory as shown in a previous section. Clearly, deviation from unity in the value of k_s, ζ, or λ_{2B} leads to residual stresses, more so when the deviation is in more than one parameter. Most importantly, these results show how the stress fields in the skin could potentially change as a result of wound healing (Swain and Gupta, 2015). This is expected since, while healing is in progress, the cellular processes at the skin edge exert internal forces which are primarily responsible for such changes. Moreover, when applied stretch is considered (blue lines), the magnitude of residual stresses is the highest whereas the wrinkling radius minimum. It should be noted that we have ignored the natural pre-tension of the skin while plotting these stresses, which should otherwise be superimposed with the obtained residual stresses to find the total stress distribution. In the following subsections we further elaborate the role of various parameters on wrinkling, wound edge stresses, rupture of wound, and critical stretch for void formation.

4.1. Role of applied stretch at the outer edge of the skin

The stretching of skin can occur due to normal motion of the body (of various joints, muscles, and limb), change in postures, or even due to respiration and neck movements. It could be severe if skin rubs along with external objects or if the body experiences sudden motion as in sports. The severity of stretching is captured by the variable λ_{2B} in our model. The effects of stretching on wrinkling, stress distribution, and cavitation are summarized in Fig. 6 and Table 1(a). The dashed lines in Fig. 6 are the tension field solutions while the solid lines are obtained without incorporating tension field. Expectedly, wrinkling decreases the magnitude of radial stresses due to the lateral slackening. Our results also show that the wrinkled region diminishes with increased radial stretching. This is due to increased tensile stresses in the skin owing to higher boundary stretching. The stresses at the wound edge are also proportional to the applied stretch. An increase in applied stretch may therefore lead to sudden void formation and subsequent rupturing in wounds whose shear modulus is less than 0.9 times the modulus of skin. In other words, severe stretching will always lead to wound rupture. Lower values of stretching however can rupture wounds only up to specific Poisson's ratios, as shown in Table 1(a). The critical stretch behavior in Table 1(a) shows that even small amount of stretching inside the wound is sufficient for rupture whenever the externally applied stretches are large.

4.2. Role of the location of applied stretch

The applied stretch is provided at the outer edge of the skin whose location is fixed by the parameter α for a given A. The considered location may vary depending on the physical position of the wound on the body, for example wounds on knee or elbow joints are subjected to local stretching whereas wounds on chest and abdominal joints are exposed to only far field stretching. Moreover, sports related trauma in the wound can occur due to arbitrary contact of skin with external objects thereby inducing in-plane stretching. The effects of α on wrinkle characteristics, stress distribution, and cavitation are summarized in Fig. 7 and Table 1(b). A localized stretching results in smaller wrinkles due to increased stresses in the skin and at the wound edge. Moreover, localized stretching can rupture all wounds with shear moduli 0.7 times less than that of skin. When the location of applied stretch moves away from the wound the rupturing becomes restricted to specific Poisson's ratios. The critical stretch required for cavitation increases with an increase in the radius of the outer edge of the skin.

4.3. Role of healing constant

The parameter ζ represents the nature of wound healing; $\zeta < 1$ implies that the wound is undergoing healing and $\zeta > 1$ denotes an atrophic condition of the wound which could be due to nutritional deficiency, hygiene, or infection. Smaller values of ζ (below unity) indicate faster healing, for example $\zeta = 0.95$ (change in radius is 5%) implies faster contraction than $\zeta = 0.99$ (change in radius is 1%). The healing of the wound can be hastened with the help of appropriate wound treatment and proper hygiene. The effects of healing condition on wrinkling in the skin, residual stresses, and rupture behavior of the wound are reported in Fig. 8 and Table 1(c). It is seen that the wounds which heal faster create larger wrinkles around the wound. This is due to relatively larger stresses in the skin and at the wound edge. The observed wrinkling behavior agrees well with the existing literature (Cerda, 2005; Geminard et al., 2004; Swain and Gupta, 2015; Flynn and McCormack, 2008). With faster healing, say $\zeta = 0.95$, a wider range of wounds with Poisson's ratios upto 0.172 can be ruptured. However, when the healing is slow, or the wound is in atrophic condition, the cavitation can occur in wounds only for a very restricted range of material parameters. Clearly, the wounds in atrophy need larger stretching to rupture. Moreover, the critical stretch required for rupturing increases with dilapidated healing condition of the wound.

4.4. Role of incompatibility at the wound edge

The incompatibility at the wound edge controls the morphoelastic behavior of cutaneous wound closure and is directly related to generation of residual stresses in the wound-skin arrangement. In our model, the incompatibility is controlled by the difference $k_s - k_w$. In the present discussion we report the effect of k_s variation on various aspect of wound healing. The parameter k_s represents the cellular action near the wound edge on the skin side leading the skin to grow towards the wound center to achieve healing (Swain and Gupta, 2015). A large value of k_s represents higher level of cell production in the skin side of the wound edge. The wrinkling behavior, stresses, and rupture behavior for various k_s values can be seen in Fig. 9 and Table 1(d). The wrinkling radius increases marginally with an increase in k_s, leading to higher stresses. See also Fig. 5, where it is clear that k_s influences both wrinkling behavior and stresses as a result of inhomogeneous expansion. A sufficiently high value of k_s can rupture all wounds with shear modulus less than 0.7 times the skin modulus due to high values of wound edge stress. For smaller k_s values wound rupture is possible only with limited constitutive conditions. The critical stretch required for void formation decreases with k_s.

Parameter	Parameter Values	Important Parameters in Skin and Wound			
		Wrinkle radius R_c/A	Wound edge Stress T_{rr}/μ_s	Poisson's ratio ν	Critical stretch λ_c
(a) Role of applied stretch at the outer edge of skin ($B = 3A$, $\zeta = 0.95$, $k_s = 1.1$, and $\mu_w = 0.7\mu_s$)					
λ_{2B}	1.01	1.41	0.448	0.172	1.729
	1.02	1.24	0.545	0.308	1.423
	1.05	1.02	0.790	$\mu_w/\mu_s \leq 0.9$	
(b) Role of the location of the applied stretch ($\lambda_{2B} = 1.01$, $\zeta = 0.95$, $k_s = 1.1$, and $\mu_w = 0.7\mu_s$)					
$\alpha = B/A$	2	1.10	0.673	$\mu_w/\mu_s \leq 0.7$	
	3	1.41	0.448	0.172	1.729
	4	1.62	0.370	0.101	2.065
(c) Role of the healing constant ($B = 3A$, $\lambda_{2B} = 1.01$, $k_s = 1.1$, and $\mu_w = 0.7\mu_s$)					
ζ	0.95	1.41	0.448	0.172	1.729
	0.99	1.33	0.360	0.094	2.113
	1.01	1.28	0.315	0.065	2.389
(d) Role of the wound edge incompatibility ($B = 3A$, $\lambda_{2B} = 1.01$, $\zeta = 0.9$, and $\mu_w = 0.7\mu_s$)					
k_s	1.05	1.42	0.463	0.189	1.676
	1.10	1.48	0.552	0.321	1.404
	1.15	1.52	0.631	$\mu_w/\mu_s \leq 0.7$	
(e) Role of the elasticity of the wound ($B = 3A$, $\lambda_{2B} = 1.01$, $\zeta = 0.95$, and $k_s = 1.1$)					
μ_w/μ_s	0.65	1.41	0.448	0.212	1.611
	0.70	1.41	0.448	0.172	1.729
	0.75	1.41	0.448	0.142	1.844

Table 1: The effect of different parameters on wrinkling radius R_c/A, wound edge radial stresses T_{rr}/μ_s, critical stretch λ_c , and maximum allowable wound Poisson's ratio ν.

4.5. Role of elasticity of the wound

The elastic characteristic of the wound can be improved by means of medical treatment. In any case, the ultimate tensile strength of a wound remains much inferior than the skin until full healing is achieved (Ramsastry, 2005; Gál et al., 2006). The effect of wound shear modulus on the rupture characteristics is shown in Table 1(e). It is clear that both wrinkling behaviour and stress distribution remain invariant for all the cases studied. A variation in relative stiffness is therefore seen to effect only the rupturing of the wound. As shown in the table, an improvement in wound properties can restrict rupturing for a wide range of Poisson's ratio. Wounds with worse properties will of course rupture easily for a large class of wounds. The critical stretch required for void formation increases on improving the wound elasticity. Hence, stiffer wounds may not allow for rapid rupture.

4.6. Possibility of cavitation at the wound-skin interface

In Section 3.3, and the subsequent discussion, the cavitation in the circular wound membrane has been assumed to take place at the center. This leads to an axisymmetrical problem with a straightforward analytical solution. Another possibility is to look for solutions with cavitation at the interface of wound and skin. This would however result in a non-axisymmetric problem without analytical solutions. In this section, we nevertheless visit this scenario under some simplifying assumptions while restricting ourselves to only energy based arguments. For our analysis, we consider a circular disc of radius A, such that one half of the disc $(0 \leq R \leq A,\ 0 \leq \theta < \pi)$ is occupied by the wound membrane and the other half $(0 \leq R \leq A,\ \pi \leq \theta < 2\pi)$ by the skin membrane. We look for the possibility of cavitation at the center of this disc at the interface of wound and skin membranes. The solution to the resulting problem is assumed to remain axisymmetric. The total stored energy of the disc containing the wound-skin interface can be evaluated using $E = \int_0^A \pi(W_w + W_s)R\mathrm{d}R$ which, following the procedure used in Section 3.3, can be written as $E = (\pi R_o^2/2)\left((W_w + W_s) - (\lambda_1 - \lambda_2)\partial(W_w + W_s)/\partial\lambda_1\right)$, where all the fields are evaluated at $R = A$. As before, the homogeneous solution is given by $\lambda_1 = \lambda_2 = \lambda$ and the non-homogeneous cavitation solution by $\lambda_1 = \beta_A\lambda_2 = \beta_A\lambda$. The difference in stored energies due to homogeneous and non-homogeneous solution can then be estimated as $\Delta E = (\pi R_o^2/2)(C_{02}\lambda + 2\mu_s)(\beta - 1)^2/(\beta\lambda)^2$. Clearly, the non-homogeneous solution with the wound-skin interface is stable and has a lower energy than the homogeneous solution. However, since Varga membrane does not support cavitation, the cavitation will occur only in the wound side of the disc.

5. Concluding remarks

We have revisited the problem of cutaneous wound healing by incorporating wound rupture in a recently developed framework of interfacial biomechanical growth (Swain and Gupta, 2015). We proposed a novel hyperelastic strain energy to model the 2D wound membrane which allows for cavitation, unlike previously employed Varga membranes. The resulting framework predicted simultaneous occurrence of ruptured wound and wrinkled skin in a region adjacent to the wound edge. The relevant boundary value problems were solved analytically and closed form solutions obtained for deformation and stresses in skin-wound configuration. Both wrinkling and cavitation emerged as stable solutions to the bifurcation problems in nonlinear elasticity of 2D membranes. The present work can be advanced in several directions. Most importantly, experimental investigations on the constitutive nature of wound membrane can provide data for verification of the proposed hyperelastic model. On the other hand, precise experiments for measuring the residual stress distribution in the skin during wound healing can be used to fit unknown parameters in our model making it useful for practical biomedical applications. The theoretical framework of the model can also be improved, although at the cost of losing analytical solvability, by including membrane curvature, non-circular wounds, finite bending rigidity, and viscoelasticity, among other considerations.

Conflict of interest statement

The authors declared no potential conflicts of interest with respect to the research, authorship, and/or publication of this article.

Funding

This research received no specific grant from any funding agency in the public, commercial, or not-for-profit sectors.

References

Agha, R., Ogawa, R., Pietramaggiori, G., Orgill, D.P., 2011. A review of the role of mechanical forces in cutaneous wound healing. J. Surg. Res. 171, 700–708.

Ball, J.M., 1982. Discontinuous equilibrium solutions and cavitation in nonlinear elasticity. Philos. T. Roy. Soc. A 306, 557–611.

Bowden, L.G., Byrne, H.M., Maini, P.K., Moulton, D.E., 2016. A morphoelastic model for dermal wound closure. Biomech. Model Mechanobiol. 15, 663–681.

Broughton, G., Rohrich, R.R., 2005. Wounds and scars. Sel. Readings Plast. Surg. 10, 1–54.

Cerda, E., 2005. Mechanics of scars. J. Biomech. 38, 1598–1603.

Evans, N.D., Oreffo, R.O.C., Healy, E., Thurner, P.J., Man, Y.H., 2013. Epithelial mechanobiology, skin wound healing, and stem cell niche. J. Mech. Behav. Biomed. Mater. 28, 397–409.

Flynn, C., McCormack, B.A.O., 2008. A simplified model of scar contraction. J. Biomech. 41, 1582–1589.

Flynn, C., Taberner, A., Nielsen, P., 2011. Modeling the mechanical response of in vivo human skin under rich set of deformations. Ann. Biomed. Eng. 39, 1935–1946.

Gál, P., Toporcer, T., Vidinský, B., Mokrý, M., Novotný, M., Kilík, R., Jr., K.S., Gál, T., Sabo, J., 2006. Early changes in the tensile strength and morphology of primary sutured skin wounds in rats. Folia Biol. (Praha) 52, 109–115.

Geminard, J.C., Bernal, R., Melo, F., 2004. Wrinkle formations in axi-symmetrically stretched membranes. Eur. Phys. J. E Soft Matter 15, 117–126.

Grinnell, F., 1994. Fibroblasts, myofibroblasts, and wound contraction. J. Cell Biol. 124, 401–404.

Gurtner, G.C., Werner, S., Barrandon, Y., Longaker, M.T., 2008. Wound repair and regeneration. Nature 453, 314–321.

Hahler, B., 2006. Surgical wound dehiscence. Medsurg Nurs. 15, 296–300.

Hall, C.L., 2008. Modeling of Some Biological Materials using Continuum Mechanics. Ph.D. thesis. Queensland University of Technology, Australia.

Harhap, M. (Ed.), 1993. Complications of Dermatologic Surgery. Springer-Verlag Berlin.

Haughton, D.M., 1986. On non-existence of cavitation in incompressible elastic membranes. Q. J. Mech. Appl. Math. 39, 289–296.

Haughton, D.M., 1990. Cavitation in compressible elastic membranes. Int. J. Eng. Sci. 28, 163–168.

Haughton, D.M., 2001. Elastic membranes, in: Fu, Y.B., Ogden, R.W. (Eds.), Non-linear Elasticity: Theory and Applications. Cambridge University Press, pp. 233–267.

Haughton, D.M., McKay, B.A., 1995. Wrinkling of annular discs subjected to radial displacements. Int. J. Eng. Sci. 33, 335–350.

Horgan, C.O., Polignon, D.A., 1995. Cavitation in nonlinearly elastic solids: A review. ASME Appl. Mech. Rev. 48, 471–485.

Lejeune, E., Javili, A., Linder, C., 2016a. An algorithmic approach to multi-layer wrinkling. Extreme Mech. Lett. 7, 10–17.

Lejeune, E., Javili, A., Linder, C., 2016b. Understanding geometric instabilities in thin films via a multi-layer model. Soft Matter 12, 806–816.

Li, B., Wang, J.H.C., 2011. Fibroblasts and myofibroblasts in wound healing: Force generation and measurement. J. Tissue Viability 20, 108–120.

McMahon, J., Goriley, A., Tabor, M., 2010. Spontaneous cavitation in growing elastic membranes. Math. Mech. Solids 15, 57–77.

Murphy, K.E., Hall, C.L., McCue, S.W., McElwain, D.L.S., 2011. A two-compartment mechanochemical model of the roles of transforming growth factor β and tissue tension in dermal wound healing. J. Theor. Biol. 272, 145–159.

Murray, J.D., 2003. Mathematical Biology II: Spatial Models and Biomedical Applications. Springer-Verlag, New York.

Pipkin, A.C., 1986. The relaxed energy density for isotropic elastic membranes. IMA J. Appl. Math. 36, 85–99.

Ramsastry, S.S., 2005. Acute wounds. Clin. Plast. Surg. 32, 195–208.

Rodriguez, E.K., Hoger, A., McCulloch, A.D., 1994. Stress-dependent finite growth in soft elastic tissues. J. Biomech. 21, 455–467.

Singer, A.J., Clark, R.A.F., 1999. Cutaneous wound healing. New Engl. J. Med. 341, 738–746.

Steigmann, D.J., 1990. Tension-field theory. Proc. Roy. Soc. Lond. A Mat. 429, 141–173.

Steigmann, D.J., 1992. Cavitation in elastic membranes – an example. J. Elasticity 28, 277–187.

Swain, D., Gupta, A., 2015. Interfacial biological growth during closure of a cutaneous wound: Stress generation and wrinkle formation. Soft Matter 11, 6499–6508.

Taylor, M., Bertoldi, K., Steigmann, D.J., 2014. Spatial resolution of wrinkle patterns in thin elastic sheets at finite strain. J. Mech. Phys. Solids 62, 163–180.

Taylor, M., Davidovitch, B., Qiu, Z., Bertoldi, K., 2015. A comparative analysis of numerical approaches to the mechanics of elastic sheets. J. Mech. Phys. Solids 79, 92–107.

Tranquillo, R.T., Murray, J.D., 1992. Continuum model of fibroblast-driven wound contraction: inflammation-mediation. J. Theor. Biol. 158, 135–172.

Truesdell, C., Noll, W., 2004. The Non–Linear Field Theories of Mechanics, Third Edition. Springer-Verlag Berlin Heidelberg.

Wu, M., Amar, M.B., 2015. Growth and remodelling for profound circular wounds in skin. Biomech. Model Mechanobiol. 14, 357–370.

Xin-Chung, S., Chang-Jun, C., 2001. Exact solution for cavitated bifurcation for compressible hyperelastic materials. Int. J. Eng. Sci. 39, 1101–1117.

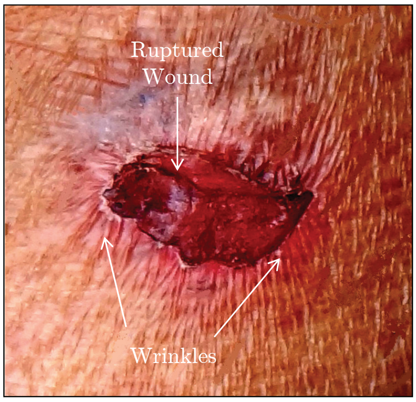

(a)

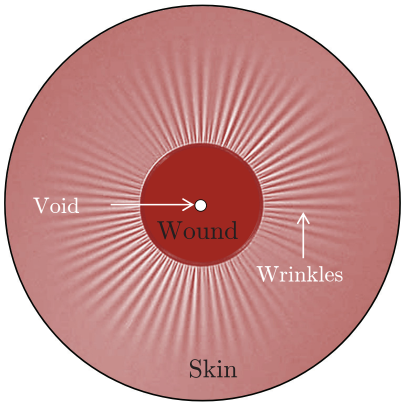

(b)

Figure 1: (a) Photograph of a ruptured wound near the knee joint surrounded by wrinkled skin. (b) Idealized representation of a ruptured wound as considered in the present work with cavitation at the center of the wound while being surrounded by an axisymmetric distribution of wrinkling in the unwounded skin.

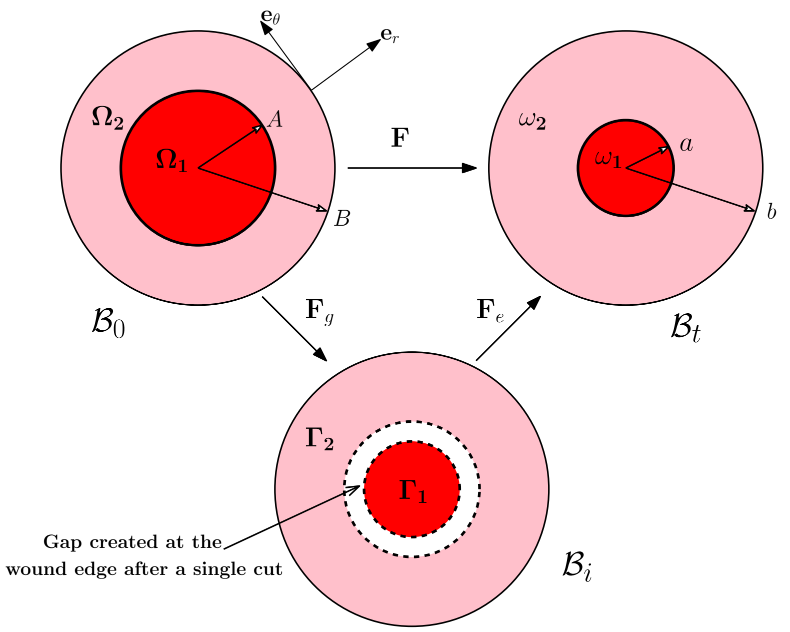

Figure 2: Kinematics of would healing, where $\mathcal{B}_0$ is the reference configuration with Ω_1 (wound) and Ω_2 (skin), $\mathcal{B}_i$ is the intermediate stress free configuration with Γ_1 (wound) and Γ_2 (skin), and $\mathcal{B}_t$ is the current configuration with ω_1 (wound) and ω_2 (skin). Figure adapted from (Swain and Gupta, 2015).

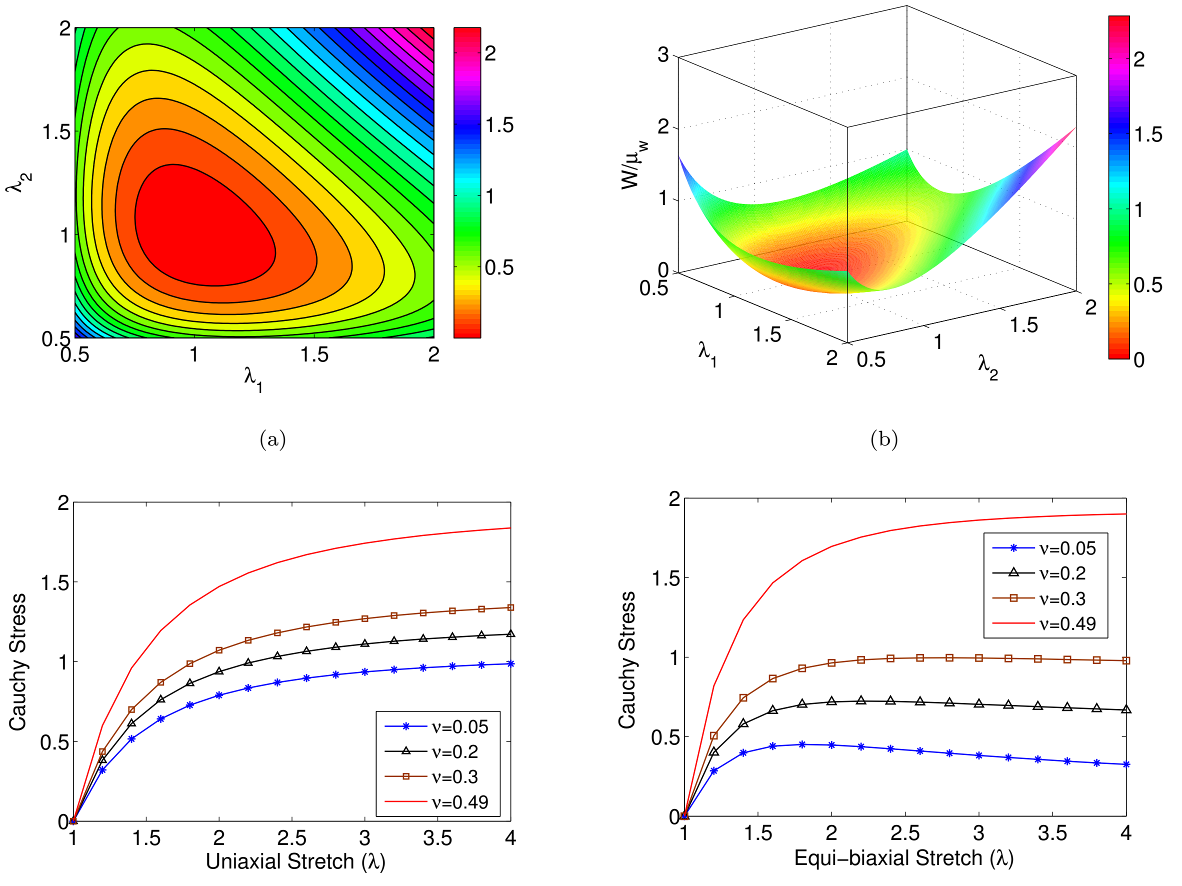

(a) (b)

(c) (d)

Figure 3: (a) Contours of the normalized SED function, W_w/μ_w, in $\lambda_1-\lambda_2$ plane with $\nu = 0.3$, (b) the same W_w/μ_w of (a) as a 3D surface plot, (c) the uniaxial stress-deformation behavior for various ν, and (d) the equi-biaxial stress-deformation behavior at various ν. The Cauchy stresses are normalized with respect to the shear modulus μ_w.

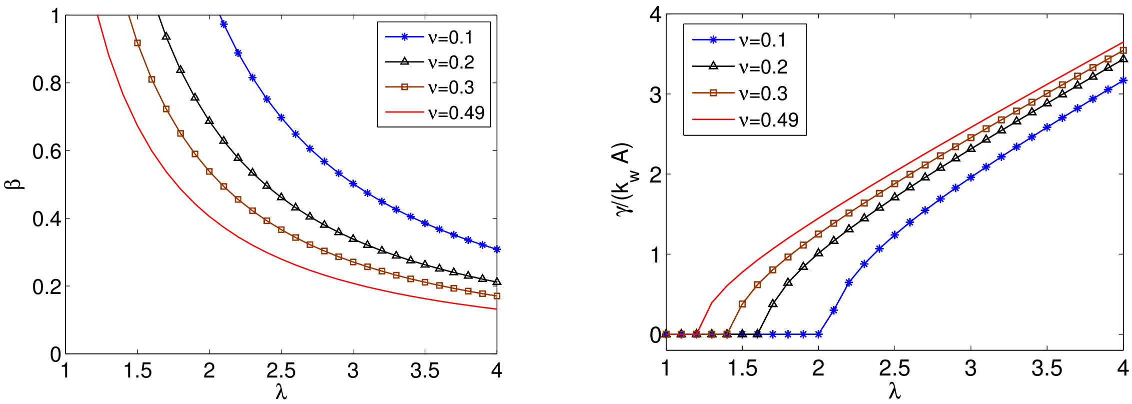

(a) (b)

Figure 4: (a) The variation of stretch ratio $\beta = \lambda_1/\lambda_2$ with applied stretch for different ν. (b) The variation of normalized void radius $\gamma/k_w A$ with applied stretch for different ν. It is only after a critical value of applied stretch that voids begin to nucleate and eventually grow into a cavity of finite size.

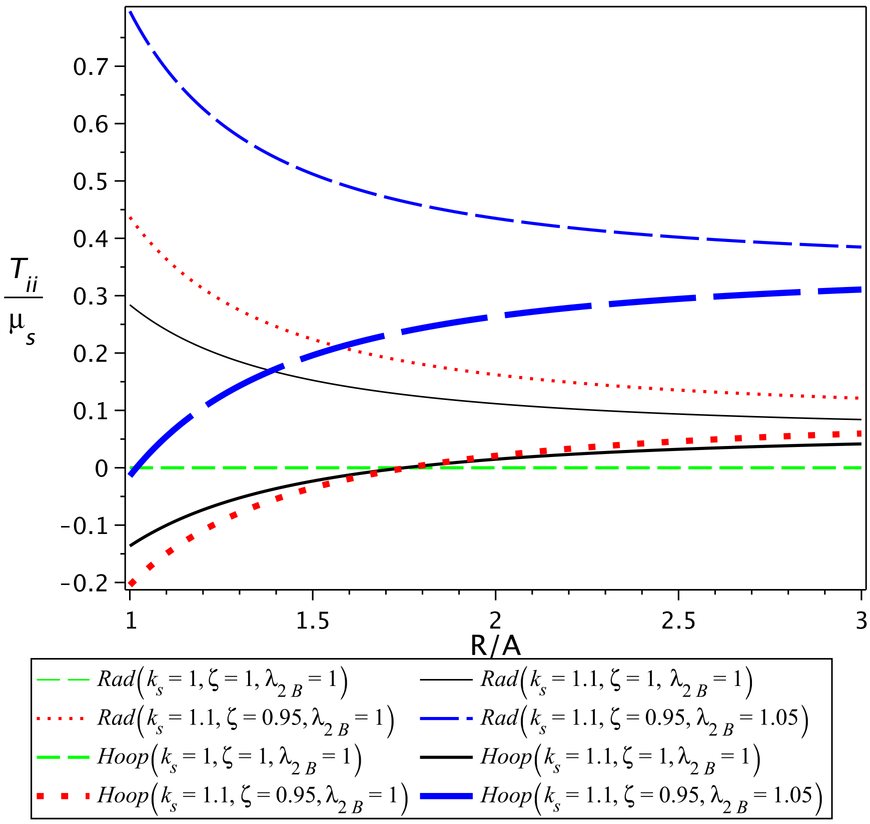

Figure 5: The normalized stresses 'T_{ii}/μ_s' are plotted for various cases of the wound-skin arrangement, where $i = r, \theta$ for radial and circumferential stresses represented as 'Rad' and 'Hoop' in the legends. The green lines indicate stresses without any stretching, healing or incompatibility, whereas black lines show the effect of incompatibility alone, red lines show the effect of incompatibility and healing, and blue lines show the effect of incompatibility, healing, and stretching together. We fix $\alpha = B/A = 3$.

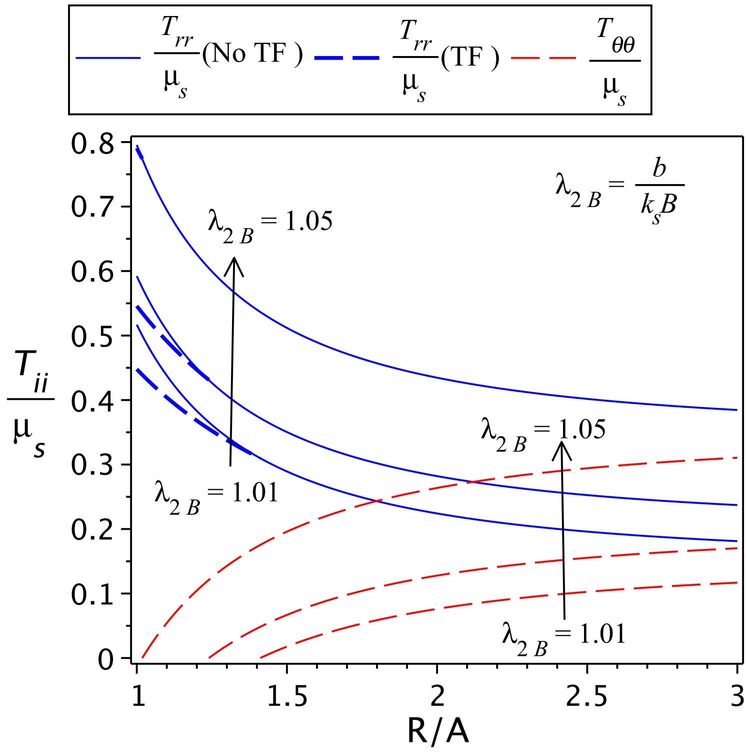

Figure 6: Normalized stresses for various applied stretches ($\lambda_{2B} = 1.01, 1.02$, and 1.05) at the outer skin edge, with $\alpha = 3$, $\zeta = 0.95$, $k_s = 1.1$, and $\mu_w = 0.7\mu_s$. The tension field (TF) solutions are shown as dashed lines.

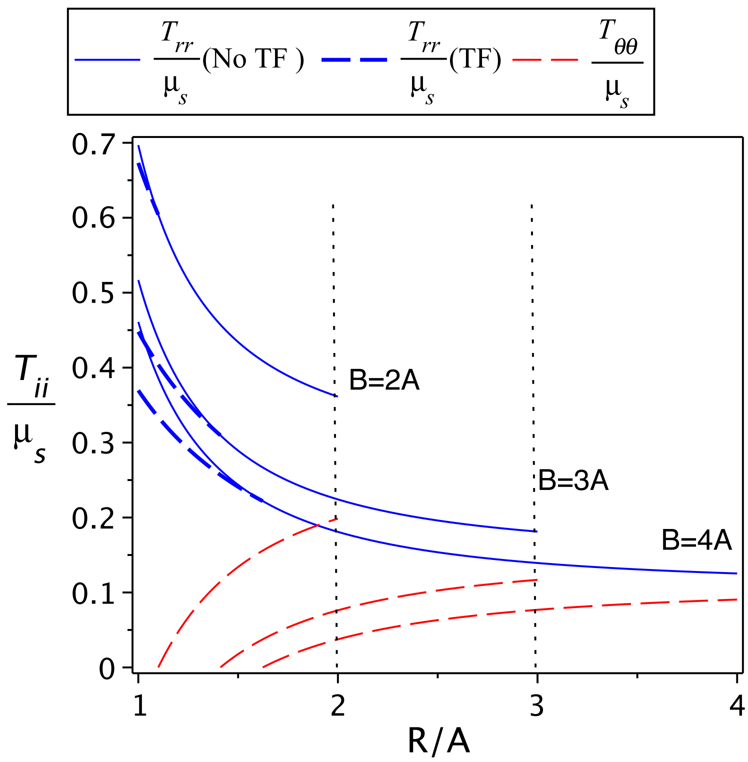

Figure 7: Normalized stresses for various positions of the applied stretch, with $\lambda_{2B} = 1.01$, $\zeta = 0.95$, $k_s = 1.1$, and $\mu_w = 0.7\mu_s$. The tension field (TF) solutions are shown as dashed lines.

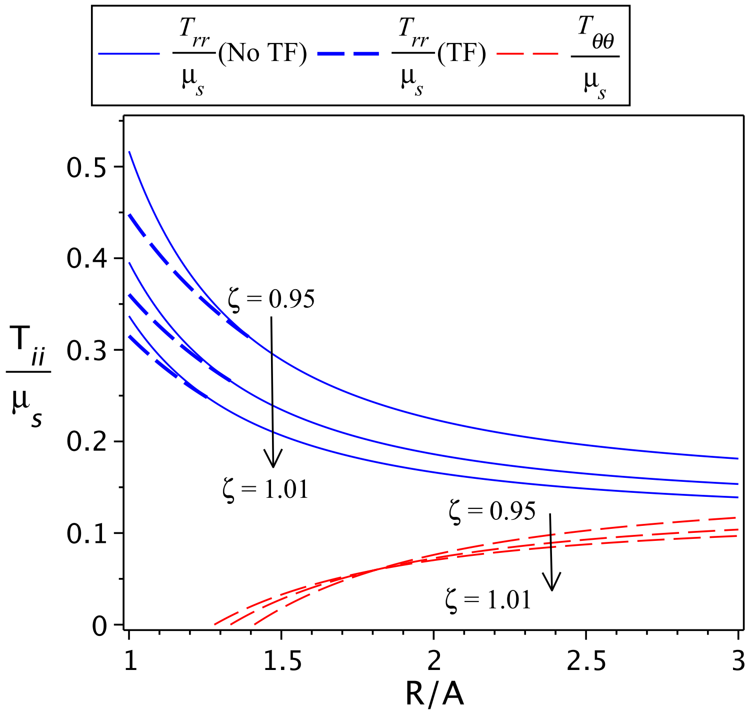

Figure 8: Normalized stresses plotted for various healing rates, where $\zeta = 0.95, 0.99$, and 1.01 represent fast healing, slow healing, and atrophy, respectively. Here, $\alpha = 3$, $\lambda_{2B} = 1.01$, $k_s = 1.1$, and $\mu_w = 0.7\mu_s$. The tension field (TF) solutions are shown as dashed lines.

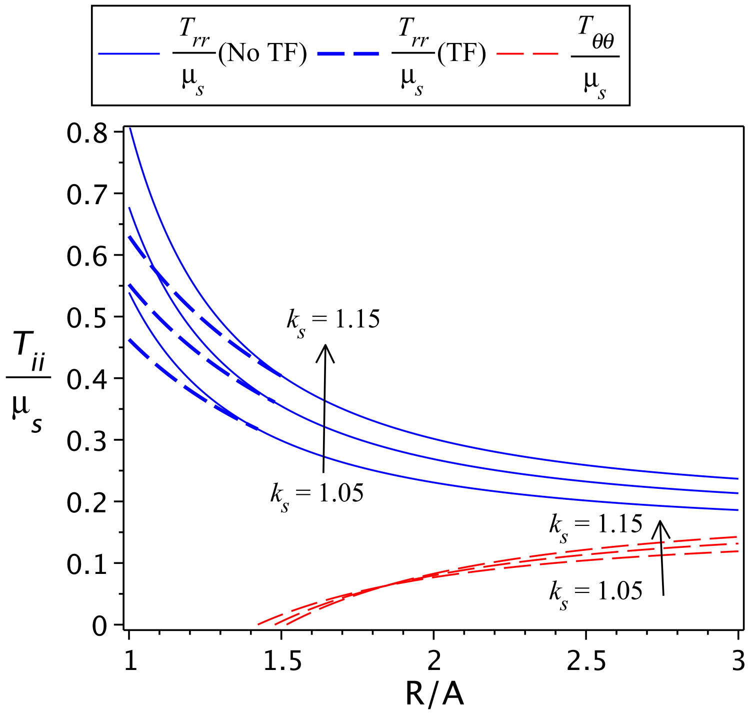

Figure 9: Normalized stresses plotted for various values of incompatibility constant ($k_s = 1.05$ (less), 1.1 (moderate), and 1.15 (high). Here, $\alpha = 3$, $\lambda_{2B} = 1.01$, $\zeta = 0.9$, and $\mu_w = 0.7\mu_s$. The tension field (TF) solutions are shown as dashed lines.